

# Surface Waves on Plasma-Clad Metal Rods

THEODOR TAMIR, SENIOR MEMBER, IEEE AND SUZANNE PALÓCZ, MEMBER, IEEE

**Summary**—Surface waves guided along a metal rod which is surrounded by a concentric isotropic plasma sheath are investigated for both the principal and the higher modes by employing a rigorous formulation. It is shown that all these modes exhibit a high frequency cutoff phenomenon; the two first modes propagate down to dc, whereas all the other modes possess a finite low frequency cut off and thus exhibit band-pass characteristics. Backward wave propagation is shown to exist when the plasma sheath is thin; dispersion curves are calculated and compared with previous data obtained by means of quasi-static approximations whose limitations and inaccuracies are also indicated. All the results are derived for the plasma-clad rod being placed either in free space or in a dielectric medium, and the dispersion features for both situations are represented in terms of universal curves.

## I. INTRODUCTION

INTEREST IN the modes guided by configurations containing an isotropic plasma medium of cylindrical shape has recently been stimulated by applications from a variety of fields. Traveling-wave tube work and electron-beam interactions with plasma have motivated the study of a simple structure, that of a circular homogeneous plasma column in free space, by Schumann<sup>1</sup> and Trivelpiece;<sup>2</sup> other, more involved configurations, were also investigated extensively by these and other workers.<sup>1-11</sup> Of particular interest is the structure of a metal cylinder which is clad by a concentric plasma sheath<sup>8,9</sup> since this may represent, under certain conditions, the idealized geometry of a missile

Manuscript received October 21, 1963. This work was sponsored by the Office of Aerospace Research (USAF), Electronics Research Directorate of the Air Force Cambridge Research Laboratories, Bedford, Mass., under contract no. AF-19(628)-2357.

Dr. Tamir is with the Electrophysics Department, Polytechnic Institute of Brooklyn, N. Y.

Mrs. Palócz is located at Pleasantville, N. Y.

<sup>1</sup> W. O. Schumann, "Über elektrische Wellen längs eines dielektrischen Zylinders in einer dielektrischen Umgebung, wobei eines oder beide der beiden Medien Plasma sind," *Z. Naturforsch.*, vol. 5a, pp. 181-191; April, 1950.

<sup>2</sup> A. W. Trivelpiece, "Slow Wave Propagation in Plasma Waveguides," *Calif. Inst. of Tech., Pasadena, Tech. Rept. No. 7*; May, 1958.

<sup>3</sup> W. O. Schumann, "Über langsame elektrische Wellen in gasgefüllten Metallrohren," *Z. Phys.*, vol. 128, pp. 629-634; December, 1950.

<sup>4</sup> L. D. Smullin and P. Chorney, "Propagation in Ion-Loaded Waveguides," *Proc. Symp. on Electronic Waveguides*, Polytechnic Institute of Brooklyn, N. Y., pp. 229-248; April, 1958.

<sup>5</sup> A. W. Trivelpiece and R. W. Gould, "Space charge waves in cylindrical plasma columns," *J. Appl. Phys.*, vol. 30, pp. 1784-1793; November, 1959.

<sup>6</sup> W. O. Schumann, "Über die Entstehung einer 'Backward Wave' in einem nichtmagnetisierten, von Luft begrenzten Plasmazylinder," *Z. angew Phys.*, vol. 12, pp. 145-148; April, 1960.

<sup>7</sup> W. O. Schumann, "Über der Einfluss der Langmuir-Schicht Zwischen Plasma und Gefäßwand auf die Wellenausbreitung in einem Plasmakabel," *Z. angew Phys.*, vol. 12, pp. 298-300; July, 1960.

<sup>8</sup> W. V. T. Rusch, "Propagation constants of surface waves on a plasma-clad cylinder," *IRE TRANS. ON ANTENNAS AND PROPAGATION (Correspondence)*, vol. AP-10, pp. 213-214; March, 1962.

<sup>9</sup> S. F. Paik, "A backward wave in plasma waveguide," *Proc. IRE (Correspondence)*, vol. 50, pp. 462-463; April, 1962.

<sup>10</sup> S. F. Paik, "Backward waves in annular plasma columns," *J. Electronics and Controls*, vol. XIII, pp. 515-524; December, 1962.

<sup>11</sup> V. I. Granatstein, S. P. Schlesinger and A. Vigants, "The open plasma guide in extremes of magnetic field," *IEEE TRANS. ON ANTENNAS AND PROPAGATION*, vol. AP-11, pp. 489-496; July, 1963.

surrounded by an ionized layer. The longitudinal modes of propagation in this case are in the form of surface waves and they are of special importance in problems concerned with waves that are excited by sources in the vicinity of the guiding structure.

The present paper examines in detail the surface waves guided by a plasma-clad metal rod and investigates their properties for both the principal *E*-type mode and for the higher hybrid modes. It is observed that the structure studied here is essentially a Goubau line<sup>12,13</sup> in which the dielectric has been replaced by plasma. Due to the dispersive character of the latter medium, the behavior of surface waves along the plasma Goubau line is markedly different from that of waves along the dielectric Goubau line.

One such an aspect is that, in certain ranges, the surface wave along the plasma line has a backward-wave character, as already shown by Paik,<sup>9,10</sup> however, he only considered the principal, circular-symmetric mode and obtained results by using an approximate quasi-static method which is permissible for a certain range of parameters. Rusch<sup>8</sup> used a rigorous analysis and examined both the principal and the first higher modes but found no backward-wave behavior; in his case, the absence of the backward wave is due to the fact that he did not look for solutions in the entire frequency range for which propagation is possible, and he employed values of the geometric and physical parameters for which only surface waves of the usual forward type are possible. On the other hand, it is shown herein, by using a rigorous formulation, that backward waves may exist for all propagating modes whenever a suitable combination of parameters is chosen. Also, it is shown that the dispersion curves for the surface waves, as well as their possible backward character, are strongly influenced by factors which are disregarded in the quasi-static analysis used by others.<sup>2,9</sup>

Due to the dispersive character of the plasma medium, the plasma Goubau guide is shown to possess a finite *high-frequency* cutoff; this feature, a common one for plasma configurations of this type,<sup>2</sup> is obviously absent in the dielectric Goubau line since this latter contains no dispersive media. On the other hand, the two guides are similar at lower frequencies; in both cases, the first two modes propagate down to  $\omega=0$  and all the higher modes possess a finite *low-frequency* cutoff.

The special case of a vanishingly small diameter for the central metal rod is also considered and it is shown

<sup>12</sup> G. Goubau, "Surface waves and their applications to transmission lines," *J. Appl. Phys.*, vol. 21, pp. 1119-1128; November, 1950.

<sup>13</sup> H. Kikuchi and E. Yamashita, "Theory of Dielectric Waveguides and Some Experiments at 50 KMC/sec," *Proc. Symp. on Millimeter Waves*, Polytechnic Institute of Brooklyn, N. Y., pp. 619-638; April, 1959.

that, when the plasma outer diameter is very large as compared to the inner one, the modes become similar (and, in the limit, they become identical) to those along a plasma column with no metal core. This plasma column structure was examined in detail by Granatstein, Schlesinger, and Vigants<sup>11</sup> who also used rigorous methods; the present paper, therefore, extends some of their results to a more general case.

These results are further generalized by considering the effect of placing the Goubau line in an ideal dielectric rather than in free space. This is illustrated by comparing the dispersion curves for the free space and dielectric cases and it is shown that the backward-wave region is more pronounced in the latter situation.

The dispersion relations are derived in Section II and their general properties are discussed in Section III. The plasma Goubau guide in free space is then treated in Section IV, and its features are illustrated by dispersion curves which were plotted for a variety of parameters. These dispersion curves are shown in Section V to represent universal curves which are applicable for any dielectric medium surrounding the plasma guide; examples are given for a specific dielectric and comparisons are made with the free-space case.

## II. DERIVATION OF THE DISPERSION RELATION

The uniform cross section of the plasma guide is shown in Fig. 1 in which a perfectly conducting metal rod of radius  $a$  is concentrically surrounded by a plasma sheath with an outer radius  $b$ . A cylindrical coordinate system  $r, \phi, z$  is used, with the  $z$  axis taken along the axis of symmetry of the system. The medium at  $r > b$ , *i.e.*, outside the plasma, is taken to be an ideal dielectric with a relative dielectric constant  $\epsilon_r$  and the permeability is taken to be that of free space:  $\mu = \mu_0$  everywhere.

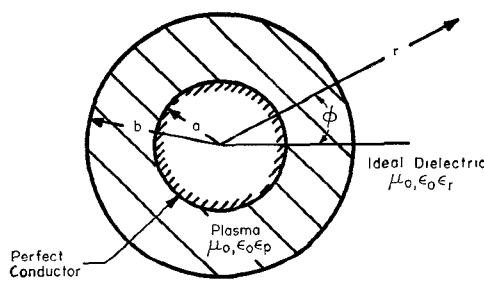


Fig. 1—Geometry of the plasma-clad metal rod.

The plasma medium at  $a < r < b$  is assumed to be uniform, isotropic and lossless; it may therefore be characterized by the relative dielectric constant

$$\epsilon_p = 1 - \left( \frac{\omega_p}{\omega} \right)^2. \quad (1)$$

The configuration described above is therefore that of a Goubau line<sup>12,13</sup> in which the dielectric at  $a < r < b$  has a permittivity of  $\epsilon_0 \epsilon_p$  and the medium at  $r > b$  is assumed,

for generality, to possess a permittivity of  $\epsilon_0 \epsilon_r$ , with  $\epsilon_0$  denoting the permittivity of free space. Hence, one may apply the characteristic equation for the Goubau line (*e.g.*, the equation derived by Kikuchi and Yamashita<sup>13</sup>) directly to the case under consideration, provided proper modifications are taken care of. We shall therefore indicate briefly the procedure for obtaining the characteristic equation and emphasize only those details for which the derivation here differs from that for the conventional Goubau line.

The surface wave modes required are characterized by a real wavenumber  $\beta$  in the  $z$  direction. One may then denote the separation variables in the radial direction by  $p$  and  $q$  for the plasma and dielectric regions, respectively; the relation between these variables is given by

$$p^2 = (\beta b)^2 - (k_0 b)^2 \epsilon_p \quad (2)$$

$$q^2 = (\beta b)^2 - (k_0 b)^2 \epsilon_r, \quad (3)$$

where  $k_0 = \omega(\mu_0 \epsilon_0)^{1/2}$  is the wavenumber of plane waves in free space.

As defined here,  $q$  is taken as a real number in order to yield field solutions which decay away from the plasma-dielectric interface at  $r = b$ , as required for a surface wave. By subtracting (3) from (2), one gets

$$p^2 = q^2 + (k_0 b)^2 (\epsilon_r - \epsilon_p), \quad (4)$$

and since  $\epsilon_r > 1 > \epsilon_p$ ,  $p$  turns out to be also real. As a consequence, the fields decay away from the plasma-dielectric interface also in the plasma region. This behavior is different from that in the conventional Goubau line where the surface wave fields decay away only in the outside ( $r > b$ ) region but are described within  $a < r < b$  by cylindrical oscillatory functions rather than the monotonically decreasing functions discussed below.

With the variables defined above, the fields may be computed by stipulating electric and magnetic longitudinal components in the form

a) in the plasma region ( $a < r < b$ ),

$$E_{zp} = \left[ A I_n \left( p \frac{r}{b} \right) + B K_n \left( p \frac{r}{b} \right) \right] e^{j(\omega t - \beta z + n\phi)} \quad (5a)$$

$$H_{zp} = \left[ C I_n \left( p \frac{r}{b} \right) + D K_n \left( p \frac{r}{b} \right) \right] e^{j(\omega t - \beta z + n\phi)}; \quad (5b)$$

b) in the outside dielectric region ( $r > b$ ),

$$E_{zq} = E K_n \left( q \frac{r}{b} \right) e^{j(\omega t - \beta z + n\phi)} \quad (6a)$$

$$H_{zq} = F K_n \left( q \frac{r}{b} \right) e^{j(\omega t - \beta z + n\phi)}, \quad (6b)$$

where  $I_n$  and  $K_n$  are, respectively,  $n$ th order Bessel functions of first and third kind with imaginary arguments. The parameter  $n$  denotes the angular variation and is

therefore an integer. One notes that, since the functions  $I_n$  and  $K_n$  are monotonic, the modes are designated here by  $n$  as a single parameter; this should be contrasted to the modes of the conventional Goubau line which are denoted by two numbers. The latter situation is due to the oscillatory nature of the Bessel functions  $J_n$  and  $N_n$  which replace the functions  $I_n$  and  $K_n$  considered here.

The characteristic (secular) equation is obtained by applying Maxwell's equations to yield all the other field components in terms of  $E_z$  and  $H_z$  and stipulating the boundary conditions

$$\begin{aligned} E_{zp} &= E_{\phi p} = 0 & \text{at } r = a \\ E_{zp} &= E_{zq}; \quad H_{zp} = H_{zq} \\ E_{\phi p} &= E_{\phi q}; \quad H_{\phi p} = H_{\phi q} \end{aligned} \quad \text{at } r = b. \quad (7)$$

Eq. (7) yields six homogeneous equations for the coefficient  $A$  to  $F$  in (5)–(6). The characteristic modes are then found by requiring the vanishing of the determinant of these six relations, thus obtaining the secular equation

$$\left[ n \frac{\beta}{k_0} \cdot \frac{p^2 - q^2}{p^2 q^2} \right]^2 = \left[ \frac{K_n'(q)}{q K_n(q)} - \frac{\gamma_4(p)}{p \gamma_2(p)} \right] \times \left[ \epsilon_r \frac{K_n'(q)}{q K_n(q)} - \epsilon_p \frac{\gamma_3(p)}{p \gamma_1(p)} \right], \quad (8)$$

where:

$$\begin{aligned} \gamma_1(p) &= K_n(p) I_n(Rp) - I_n(p) K_n(Rp) < 0, \\ \gamma_2(p) &= K_n(p) I_n'(Rp) - I_n(p) K_n'(Rp) > 0, \\ \gamma_3(p) &= K_n'(p) I_n(Rp) - I_n'(p) K_n(Rp) < 0, \\ \gamma_4(p) &= K_n'(p) I_n'(Rp) - I_n'(p) K_n'(Rp) > 0, \end{aligned} \quad (9)$$

and  $R = a/b$  is the ratio between the two radii;  $I_n'$  and  $K_n'$  are first derivatives of  $I_n$  and  $K_n$ , respectively, with respect to the *entire* argument and evaluated at  $p$  or  $Rp$  as indicated above.

To find the characteristic modes, one must find values of  $p$ ,  $q$ ,  $\beta$ , and  $k_0$  which satisfy (1), (2), (3) and (8), in terms of given values for  $\omega_p$ ,  $b$ ,  $\epsilon_r$  and  $R = a/b$ . Some simplification occurs if one solves for  $\beta$  and  $k_0$  from (2) and (3) and substitutes into (8) to obtain

$$\frac{\epsilon_p}{\epsilon_r} = \frac{\left[ \frac{K_n'(q)}{q K_n(q)} - \frac{\gamma_4(p)}{p \gamma_2(p)} \right] \cdot \frac{K_n'(q)}{q K_n(q)} - \left( \frac{n \Lambda}{p q^2} \right)^2}{\left[ \frac{K_n'(q)}{q K_n(q)} - \frac{\gamma_4(p)}{p \gamma_2(p)} \right] \cdot \frac{\gamma_3(p)}{p \gamma_1(p)} - \left( \frac{n \Lambda}{p^2 q} \right)^2}, \quad (10)$$

where

$$\Lambda^2 = p^2 - q^2 = (k_0 b)^2 (\epsilon_r - \epsilon_p). \quad (11)$$

As in the case of the conventional Goubau line, all the modes are hybrid with the exception of the principal mode (for  $n=0$ ) which is an  $E$  mode with  $H_z = H_r = E_\phi = 0$ . For the latter case, (10) reduces to

$$\frac{\epsilon_p}{\epsilon_r} = \frac{p}{q} \cdot \frac{K_0(p) I_0(Rp) - I_0(p) K_0(Rp)}{K_1(p) I_0(Rp) + I_1(p) K_0(Rp)} \cdot \frac{K_1(q)}{K_0(q)}. \quad (12)$$

Some general properties of the solutions of the characteristic equations are considered in the next section.

### III. GENERAL PROPERTIES OF THE SURFACE WAVES

Before obtaining actual dispersion curves, it is worthwhile to determine certain general features pertaining to the surface wave modes.

One notes first that the parameter  $R = a/b$  which enters into (10) by way of the  $\gamma(p)$  functions in (9) has a range of  $0 \leq R < 1$ . The limit  $R = 1$  corresponds to the plasma medium being absent; no solutions then exist since surface waves are not supported by a perfectly conducting rod. At the other extreme,  $R = 0$  refers to an infinitesimally thin metal core. One therefore expects that, as  $R \rightarrow 0$ , some of the modes studied here would be identified with the modes along a plasma column (with no metal rod) which are already known.<sup>1,2,11</sup> In fact, if a limiting process is applied to (10), one obtains

$$\lim_{R \rightarrow 0} \frac{\gamma_3(p)}{\gamma_1(p)} = \lim_{R \rightarrow 0} \frac{\gamma_4(p)}{\gamma_2(p)} = \frac{I_n'(p)}{I_n(p)}.$$

Hence,

$$\begin{aligned} \lim_{R \rightarrow 0} \frac{\epsilon_p}{\epsilon_r} &= \frac{\left[ \frac{K_n'(q)}{q K_n(q)} - \frac{I_n'(p)}{p I_n(p)} \right] \frac{K_n'(q)}{q K_n(q)} - \left( \frac{n \Lambda}{p q^2} \right)^2}{\left[ \frac{K_n'(q)}{q K_n(q)} - \frac{I_n'(p)}{p I_n(p)} \right] \frac{I_n'(p)}{p I_n(p)} - \left( \frac{n \Lambda}{p^2 q} \right)^2}. \end{aligned} \quad (13)$$

However, (13) turns out to be the exact characteristic equation for the plasma column. Hence, *all* of the modes along a plasma cylinder (with no metal core) are accounted for by taking the limit case of  $R = 0$  in a plasma Goubau line.

It should be observed that the above result is not an obvious one since the limiting process above should yield only those modes for which the longitudinal electric field is zero along the axis of a plasma column. However, it so happens that the *complete* set of modes along a plasma cylinder satisfies this condition, with the exception of the principal ( $n=0$ ) mode. On the other hand, this principal mode cannot be supported by a Goubau plasma guide with  $R = 0$  unless the condition for a vanishing electric field along the axis is disregarded, in which case the guide is indistinguishable from a plasma column. The *complete* picture of the modes of the latter guide as obtainable from those of the plasma Goubau line is thus explained.

When examining the general behavior of the dispersion ( $\omega$  vs  $\beta$ ) curves that one obtains via (10), it is first observed that these curves must be restricted to a range  $\omega < \omega_p$  (*i.e.*,  $\epsilon_p < 0$ ). This is due to the fact that  $0 < \epsilon_p < 1$  for  $\omega > \omega_p$ , so that the dielectric constant of the sheath

surrounding the metal core is positive and smaller than that of the outside medium (assuming, of course, that  $\epsilon_r > 1$ ). However, surface waves are possible along such a guide only if the reverse is true, as for example, is the case for the conventional Goubau line. Hence, the dispersion curves of the plasma guide are restricted to values below.

$$\omega_1 = \omega_p. \quad (14a)$$

Another limit feature in terms of frequency is an asymptotic behavior for large wavenumbers  $\beta$ . This is obtained by noting that  $\epsilon_p$  (and hence  $\omega$ ) is a continuous and single-valued function of the parameter  $q$  (and therefore also of  $\beta b$ ). Then one can see by inspection of (2) and (3) that, as  $\beta b \rightarrow \infty$ , both  $p$  and  $q$  become very large at finite frequencies. One is therefore justified in applying the large argument approximations for the Bessel functions in (8) and (9) to get

$$\lim_{p \rightarrow \infty} \frac{\gamma_4(p)}{\gamma_2(p)} = \lim_{p \rightarrow \infty} \frac{\gamma_3(p)}{\gamma_1(p)} = 1,$$

which, when substituted into (10), yields

$$\lim_{p \rightarrow \infty} \frac{\epsilon_p}{\epsilon_r} = -1.$$

Hence, using (1) one obtains an asymptotic behavior for a frequency given by

$$\omega_2 = \frac{\omega_p}{\sqrt{1 + \epsilon_r}} \quad (14b)$$

which is a result already obtained by others<sup>1,2</sup> for a variety of other cylindrical plasma structures. As pointed out before, this asymptotic behavior is due to the dispersive qualities of the plasma medium and is not a function of geometry.

Due to the upper frequency limit imposed by  $\omega_1 = \omega_p$  and the asymptotic behavior at  $\omega_2$ , a high-frequency cutoff phenomenon must be associated with a frequency  $\omega_c$  such that  $\omega_2 \leq \omega_c \leq \omega_1$  for any mode  $n$ . It is also evident that these curves must exhibit a backward-wave region if the cutoff frequency  $\omega_c$  lies within

$$\frac{1}{\sqrt{1 + \epsilon_r}} < \frac{\omega_c}{\omega_p} \leq 1, \quad (15)$$

i.e., whenever  $\omega_c$  does not coincide with  $\omega_2$  (see, for example, the dispersion curves in the next section). The possibility of obtaining such a value of  $\omega_c$  is clarified upon viewing a planar plasma layer as another limit case for the geometry of the plasma Goubau line.

When both radii  $a$  and  $b$  become infinite in such a manner that their difference  $d = b - a$  remains finite, the geometry of the circular plasma guide degenerates into a plasma slab backed by a perfect conductor, as shown

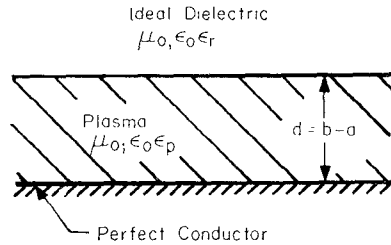


Fig. 2—Geometry of the plasma slab.

in Fig. 2. This particular geometry has already been studied,<sup>14-16</sup> and it was shown that, for  $\epsilon_r = 1$ , the surface waves may have a backward-wave character which appears for small values (less than 0.73 . . .) of the parameter  $\Lambda$  defined in (11).

To pursue this analogy further, one notes that if the plasma guide is to resemble the plasma slab of Fig. 2, it is necessary for

$$d = b - a = b(1 - R)$$

to remain finite as the radius  $b$  increases indefinitely; hence,  $R$  should be close to unity. The backward-wave character is therefore expected to appear if the conditions that  $\Lambda$  be small and  $R$  be close to unity are both satisfied. This indeed turns out to be the case, as shown in the succeeding Sections wherein the physical significance of  $\Lambda$  is also discussed. Also, the cutoff frequency  $\omega_c$  lies within  $\omega_2 < \omega_c \leq \omega_1$  when the backward-wave behavior exists, as expected.

It is clear that  $\omega_c$  represents a *high-frequency* cutoff value which is due mainly to the dispersive nature of the plasma and which does not therefore appear in the dispersion relations for the conventional (dielectric) Goubau line. One should, therefore, look for an additional cutoff phenomenon which is associated with the geometry of the given guide. This occurs at a value of  $\omega = \omega_0$  such that  $\beta = k_0 \epsilon_r$ , i.e., when the phase velocity of the surface wave equals the velocity of light in the outer medium. It then turns out (see Appendix) that this limit frequency  $\omega_0$  is finite only for modes with  $n \geq 2$ , while for both  $n = 0$  and  $n = 1$  no such cutoff occurs and propagation exists down to  $\omega = 0$ . The behavior at the lower phase velocities is therefore similar to that in the conventional Goubau line;<sup>13</sup> this is obviously due to the fact that the geometry, which determines the low phase velocity behavior, is essentially the same for both the plasma and the dielectric guides.

The mechanism of energy transport for a surface wave was already discussed for a plasma slab<sup>15</sup> and it was shown that the power travels in opposite directions in the plasma and in the outer dielectric. The surface

<sup>14</sup> A. A. Oliner and T. Tamir, "Backward waves on isotropic plasma slabs," *J. Appl. Phys.*, vol. 33, pp. 231-233; January, 1962.

<sup>15</sup> T. Tamir and A. A. Oliner, "The spectrum of electromagnetic waves guided by a plasma layer," *PROC. IEEE*, vol. 51, pp. 317-332; February, 1963.

<sup>16</sup> S. Palócz, "Backward Wave Propagation in Plasma Structures," M.S. Thesis, Dept. of Electrical Engineering, Polytechnic Institute of Brooklyn, N. Y.; June, 1963.

wave is then of the backward type if the power contents of the plasma region is larger than that of the outer dielectric region and, when the reverse is true, the wave is of the forward type. This behavior is also due to the dispersive character of the plasma medium and, in particular, to the fact that  $\epsilon_p$  has to be negative if surface waves are propagated. Although these features were not specifically examined for the present circular geometry, it is expected that the surface waves along the plasma Goubau line possess identical characteristics insofar as power features are concerned.

#### IV. DISPERSION CURVES FOR THE CASE $\epsilon_p = 1$

When the outer dielectric (at  $r > b$ ) is free space (or air), a certain simplification occurs for the secular equation (10) in that the parameter  $\Lambda$  becomes a constant. This is due to (11) which, together with (1), yields a value

$$\Lambda_0 = \frac{\omega_p b}{c} = 2\pi \frac{b}{\lambda_p}, \quad (16)$$

where  $c$  is the velocity of light and  $\lambda_p$  is the plasma wavelength. Hence, unlike the general case ( $\epsilon_p \neq 1$ ),  $\Lambda_0$  is independent of frequency and is a constant determined by geometry (through  $b$ ) and the physical condition of the medium (through  $\lambda_p$ ). Small and high values of  $\Lambda_0$  correspond, respectively, to weak and strong concentrations of electrons in the plasma region (for a fixed value of  $b$ ).

The dispersion curves may then easily be plotted by regarding  $q$  as a running variable in (10) for fixed values of parameters  $\Lambda_0$  and  $R$ ;  $p$  is simply expressed in terms of  $q$  and  $\Lambda_0$  by means of (11) and values of  $\epsilon_p$  are then found directly. This procedure lends itself easily to programming on a computer. Several curves were thus obtained with an IBM 650 computer and the results are shown in Figs. 3-5 for the first three propagating modes.

An inspection of these figures shows that all the features discussed in the preceding section are confirmed numerically. The  $R=0$  curves refer to modes along a plasma cylinder (with no metal core) and they correspond to curves already calculated by Granatstein, Schlesinger and Vigants.<sup>11</sup> As already pointed out by these authors, the principal ( $n=0$ ) surface wave is never backward although the higher modes may exhibit this feature. On the other hand, it is seen in Fig. 3 that the waves may be backward if  $R \neq 0$ , as already shown by Paik<sup>9</sup> who used an approximation which is valid in a restricted range. In addition, it is evident that the backward wave character is retained in the higher modes, as seen in Figs. 4 and 5. This feature was overlooked by Rusch<sup>8</sup> who used an exact formulation to find the dispersion curves; but did not investigate solutions in the range  $K\omega_p/\omega c J_2$  (*i.e.*,  $-1 < \epsilon_p < 0$ ).

It is also noted that the analogy with a plasma slab (see Section III) is confirmed by the curves. The backward waves, for all the modes, are most prominent when

both  $\Lambda_0$  and  $1-R$  are small and the range of the backward feature is reduced whenever one of these parameters increases.

The absence of a low-frequency cutoff for the  $n=0$  and  $n=1$  modes is observed in Figs. 3 and 4. It may be noticed in Fig. 4 that the lower-frequency region (extending at about  $\omega/\omega_p < 0.6$ ) yields phase velocities very close to the speed of light and therefore  $q$  is then extremely small. This corresponds to a wave that is very loosely bound to the plasma guide and it is doubtful whether this region could be reproduced under laboratory conditions.

The upper-frequency cutoff  $\omega_c$  is clearly apparent in all the curves. In fact, at the higher modes ( $n \geq 2$ ), one notes in Fig. 5 that  $\omega_c$  may coincide or be very close to the limit frequency  $\omega_0$  (for  $\beta = k_0 \sqrt{\epsilon_r}$ ). In that case, practically all of the propagation range has backward-wave character; also, the entire dispersion curve is then restricted to a narrow frequency band for small values of  $\Lambda_0$ .

An interesting aspect of the results shown in the figures is that the dispersion curves for large values of  $\Lambda_0$  are very similar for all the modes shown. This is explained by the fact that, for  $\Lambda_0 \gg 1$ ,  $b$  is very large when compared to  $\lambda_p$ ; also, since the frequency  $\omega$  within the propagating region is of the order of  $\omega_p$ , it follows that this is a case of a guide operating at relatively high frequencies so that the dispersion curves for successive modes are indeed expected to be close to each other.

The fact that  $b \gg \lambda_p$  if  $\Lambda_0 \gg 1$  also explains the proximity of the  $R=0$  and  $R=0.9$  curves for  $\Lambda_0=10$ . The difference between any two curves with different values of  $R$  is caused by the presence of the metal core; however, due to (11), the decay of the wave within the plasma region is very strong for large values of  $\Lambda_0$ , so that the presence of the metal is not felt in those cases unless the plasma sheath is thin (*i.e.*,  $R$  is close to unity). The reverse is evidently true for smaller values of  $\Lambda_0$ ; in those cases, the metal core influences propagation even for small values of  $R$  since then the plasma sheath is thin in terms of the plasma wavelength  $\lambda_p$ .

To facilitate certain calculations, the phase velocity is shown in Figs. 3-5 by means of dashed lines. In particular, one may estimate the ranges of validity for the quasi-static approximations that were previously used in treating similar problems.<sup>2,9</sup>

It is interesting to observe that the curves shown here exhibit clearly the role played by the variable  $\Lambda_0$  whereas the quasi-static analysis does not take this parameter into account at all. This is due to the fact that the approximate quasi-static method assumes that the variables  $p$  and  $q$  are very close to each other. This will hold for a large frequency range only if  $\Lambda_0$  is small. Hence, the quasi-static analysis will always yield results that are similar with the curves for  $\Lambda_0=0.1$ , of Figs. 3-5. For larger values of  $\Lambda_0$ , this approximation may lead to erroneous results; thus, for  $\Lambda_0=10$  and  $R=0.1-0.9$ , the quasi-static method would show a backward wave region

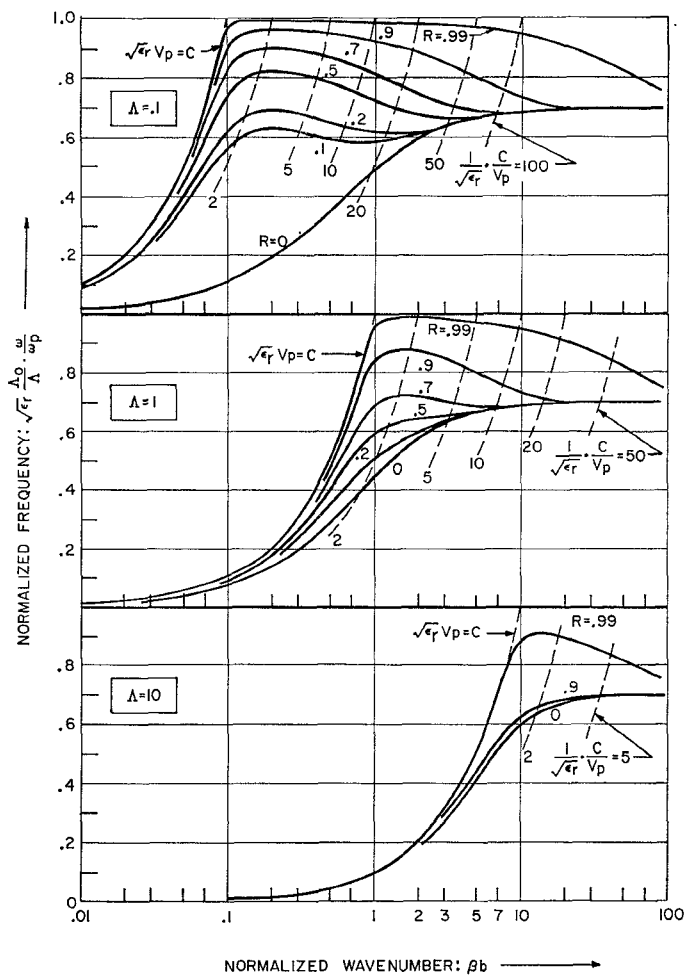


Fig. 3—Universal dispersion curves for the principal (circularly symmetric) mode ( $n=0$ ).  $R=a/b$ ,  $V_p$ =phase velocity,  $P_c$ =speed of light in vacuum. When the outer medium is free space,  $\epsilon_r=1$  and  $\Delta=\Delta_0=\omega_p b/c=2\pi b/\lambda_p$ .

which is decidedly nonexistent, as indicated by the curves obtained rigorously and shown here in Figs. 3-5.

#### V. DISPERSION CURVES FOR THE GENERAL CASE $\epsilon_r \neq 1$

Whereas the outer medium (at  $r>b$ ) was taken as air or free space in the previous section, it is also interesting to obtain dispersion curves for the more general case of an outer ideal dielectric. Thus, when the plasma sheath is enclosed by a glass cylinder, the modes of propagation may be found by considering glass rather than air as the outer medium. The fact that the surface waves are decaying away from the plasma-glass interface will justify the approximation involved in neglecting the air region surrounding the glass, at least in the case of sufficiently thick glass walls.

To obtain dispersion curves for  $\epsilon_r \neq 1$ , one observes that, by eliminating  $k_0 b$  in (2) and (3) and using the definition for  $\Lambda$  in (11), one obtains:

$$(\beta b)^2 = q^2 + \frac{\Lambda^2}{1 - \frac{\epsilon_p}{\epsilon_r}}. \quad (17)$$

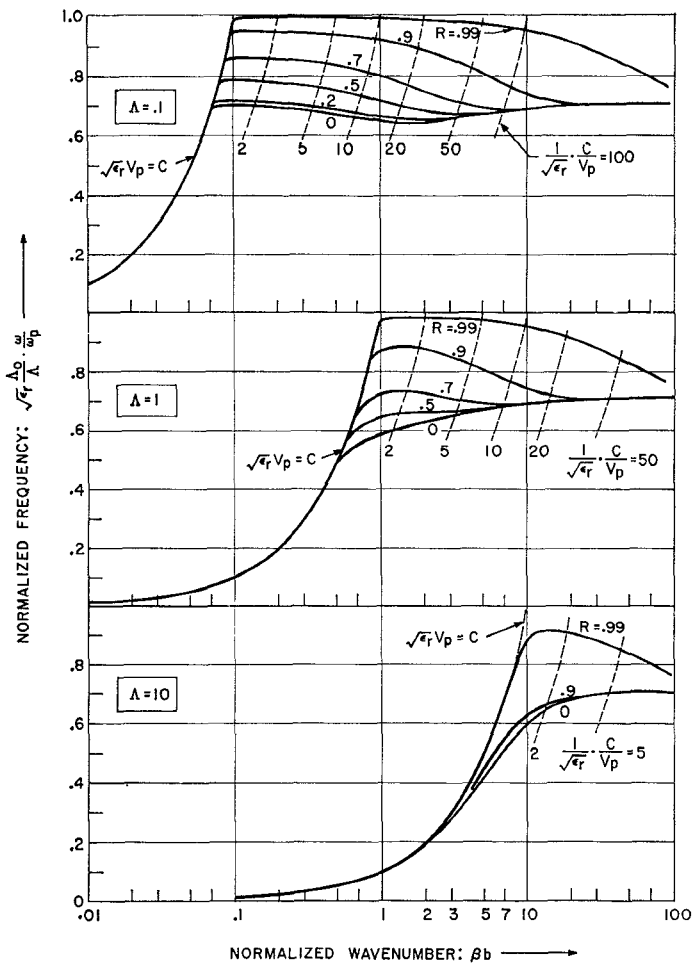


Fig. 4—Universal dispersion curves for the first hybrid mode ( $n=1$ ).  $R=a/b$ ,  $V_p$ =phase velocity,  $c$ =speed of light in vacuum. When the outer medium is free space,  $\epsilon_r=1$  and  $\Delta=\Delta_0=\omega_p b/c=2\pi b/\lambda_p$ .

However, the characteristic equation (10) shows that the ratio  $\epsilon_p/\epsilon_r$  is independent of  $\epsilon_r$  for any given combination of the parameters  $n$ ,  $R$ ,  $q$  and  $\Lambda$ ; hence  $\beta b$  itself is not dependent on any particular  $\epsilon_r$  under the same conditions.

The parameter  $\Lambda$  does not have a simple physical meaning except in the particular case of free space, as described in the previous section. On the other hand, (11) may be written as

$$\Lambda^2 = \left( \frac{\omega_p b}{c} \right)^2 \left( \frac{\omega}{\omega_p} \right)^2 (\epsilon_r - \epsilon_p) = \left( \Lambda_0 \frac{\omega}{\omega_p} \right)^2 (\epsilon_r - \epsilon_p),$$

which, by using expression (1) for  $\epsilon_p$ , yields

$$\left( \frac{\Lambda}{\Lambda_0} \right)^2 = 1 + (\epsilon_r - 1) \left( \frac{\omega}{\omega_p} \right)^2. \quad (18)$$

Consider now the ordinate  $y$  used in Figs. 3-5. By substituting (18), one gets

$$y = \sqrt{\epsilon_r} \frac{\Lambda_0}{\Lambda} \frac{\omega}{\omega_p} = \left( 1 - \frac{\epsilon_p}{\epsilon_r} \right)^{-\frac{1}{2}}, \quad (19)$$

which, by virtue of the argument employed above, is not a function of  $\epsilon_r$ .

One therefore observes that, for any point on the dis-

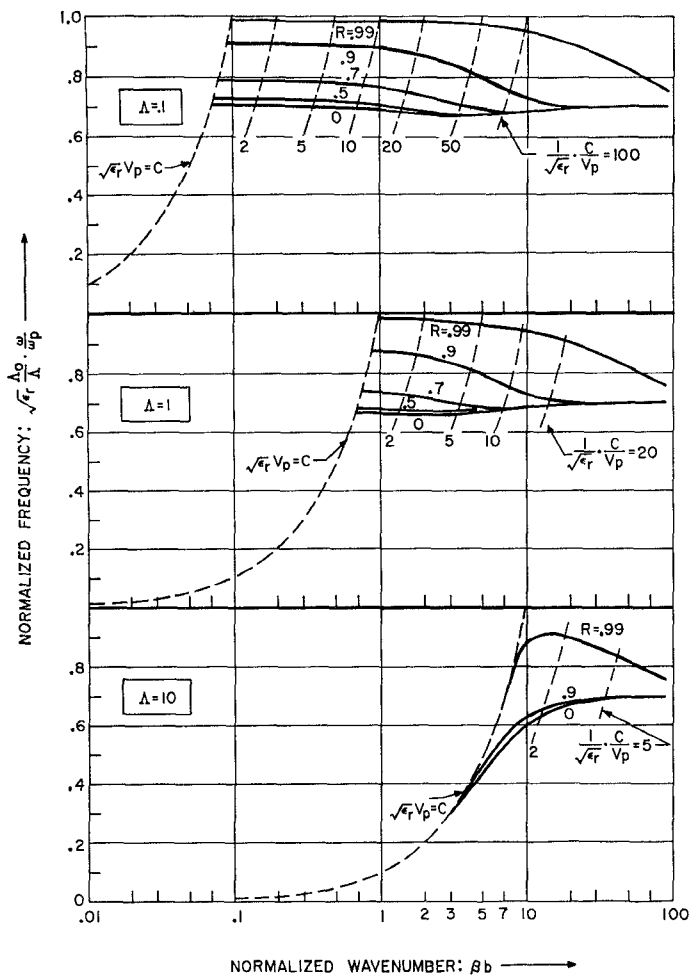


Fig. 5—Universal dispersion curves for the second hybrid mode ( $n=2$ ).  $R=a/b$ ,  $v_p$  = phase velocity,  $c$  = speed of light in vacuum. When the outer medium is free space:  $\epsilon_r=1$  and  $\Lambda=\Lambda_0=\omega_p b/c=2\pi b/\lambda_p$ .

dispersion curves, both the abscissa  $\beta b$  and the ordinate  $y$  are entirely independent of the value of  $\epsilon_r$ . Hence, Figs. 3-5 represent universal curves for any  $\epsilon_r$ ; the dielectric constant in the outer medium is, for any  $\beta b$ , reflected only in the values of  $\omega/\omega_p$  as obtained by means of the curves and the use of (18) and (19).

Although the universal curves in Figs. 3-5 are useful in finding the appropriate wavenumber  $\beta$  for any given geometry and operating frequency, the graphs do not show dispersion curves in the usual sense since, if  $\epsilon_r \neq 1$ , the parameter  $\Lambda$  itself is not constant with frequency. It is, however, easy to plot any dispersion curve (with  $\Lambda_0 = \text{constant}$  rather than  $\Lambda = \text{constant}$ ) by using the given universal curves in conjunction with (18) and (19). This is illustrated in Fig. 6 which was constructed with the aid of universal curves shown in Fig. 3 and with the pertinent relations (18) and (19).

A significant feature of the dispersion curves for  $\epsilon_r \neq 1$  is that the backward-wave region may be appreciably wider when compared to the free-space case  $\epsilon_r = 1$ . This is due to the fact that the dispersion relations are dominated by the geometry at lower values of  $\beta b$  and by the dielectric region at higher values of  $\beta b$ . In the latter case, the curves approach the asymptote at

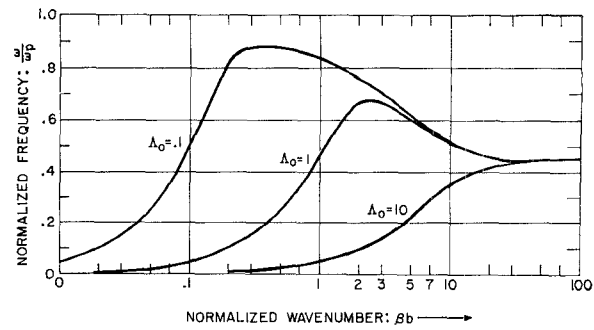


Fig. 6—Dispersion curves for the principal mode ( $n=0$ ), with:  $R=0.9$  and  $\epsilon_r=4$ .

$$\frac{\omega}{\omega_p} = \frac{1}{\sqrt{1+\epsilon_r}},$$

already derived in Section III. At the lower values of  $\beta b$ , the curves reach frequencies close to  $\omega/\omega_p=1$ , especially for the smaller values of  $\Lambda_0$ ; also, varying  $\epsilon_r$  has little effect on the maximum attainable value of  $\omega/\omega_p$ .

The resulting increase of the bandwidth for the backward-wave region may be seen by comparing Figs. 3 and 6; in particular, for  $\Lambda_0=0.1$ , the bandwidth for  $\epsilon_r=4$  is nearly twice that for  $\epsilon_r=1$ . It is evident that a more pronounced increase in the backward-wave bandwidth may be achieved by increasing  $R$  or  $\epsilon_r$ , or both.

At the end of Section IV, a comparison was made between the quasi-static approximation and the present rigorous method for obtaining dispersion curves and the significance of the parameter  $\Lambda_0$  was demonstrated. It is clear that all these comments also apply for the case  $\epsilon_r \neq 1$  since the curves discussed here are derived directly from the ones in the previous section.

## VI. CONCLUSION

The modes supported by a plasma Goubau line were examined in detail and it was shown that backward-wave propagation regions may exist for both the principal  $E$ -type mode and the higher hybrid modes. The condition for the existence of these regions was found to be that the diameter of the metal core must be large when compared to the thickness of the plasma sheath, but small when compared to the plasma wavelength  $\lambda_p$ .

The backward-wave range may be considerably enhanced by surrounding the plasma sheath with a dielectric medium rather than free space.

The behavior at small phase velocities is determined mainly by the geometry of the guide. Due to this reason, both the plasma and the dielectric Goubau lines are similar in that the first two modes propagate down to  $\omega=0$ , whereas all the higher modes possess a finite limiting frequency. On the other hand, the dispersive nature of the plasma manifests itself at the higher phase velocities and introduces a high-frequency cutoff phenomenon which is absent in the conventional Goubau line. The propagation range for the higher modes is therefore restricted to a frequency band which may become very narrow for a suitable choice of the parameters involved.

In view of the above characteristics, the plasma Goubau line offers possibilities as a band filter application or as a means for developing a simple slow backward-wave structure. In addition, the various surface wave modes analyzed herein are of importance in problems involving radiation from missiles which are surrounded by an ionized layer when they reenter the atmosphere.

Although the analysis here is rigorous, it is also recognized that the plasma is taken as a highly idealized medium which may not be appropriate for the applications cited above. Thus, losses due to collisions or other causes were disregarded and the plasma was taken as a completely uniform medium which is sharply defined in space. It is nevertheless expected that the main features described here (such as the existence itself of surface waves and their backward-wave character) will be retained even in actual, less perfect, plasma configurations.

### VII. APPENDIX—CALCULATION OF THE LIMIT FREQUENCY $\omega_0$

The values for the limit frequency  $\omega_0$  are obtained by letting  $q$  approach zero in (10) or (12). One then distinguishes between the following situations.

a)  $n=0$

In this case, (12) is used and, since  $p \rightarrow \Lambda$  as  $q \rightarrow 0$ , it is seen by inspection that  $\epsilon_p \rightarrow -\infty$ . This means that  $\omega/\omega_p \rightarrow 0$  so that propagation extends to dc in the principal mode.

b)  $n=1$

For the first hybrid mode, (10) is employed together with the following approximation for the Bessel functions of small arguments.

$$\frac{K_1'(q)}{qK_1(q)} \approx -\frac{1}{q^2} \left( 1 - q^2 \log \frac{\gamma q}{2} \right),$$

where  $C = \log \gamma = 0.5772 \dots$  is Euler's constant. Multiplying the numerator and denominator of (10) with  $q^4$ , introducing the above approximation and retaining first terms only, one obtains for very small values of  $q$

$$\frac{\epsilon_p}{\epsilon_r} \rightarrow \frac{\frac{2\Lambda \log \frac{\gamma q}{2} - \left[ \frac{1}{\Lambda} + \frac{\gamma_4(\Lambda)}{\gamma_2(\Lambda)} \right]}{\frac{1}{\Lambda} + \frac{\gamma_3(\Lambda)}{\gamma_1(\Lambda)}}}{\frac{1}{\Lambda} + \frac{\gamma_3(\Lambda)}{\gamma_1(\Lambda)}}.$$

Due to the term containing the logarithm,  $\epsilon_p \rightarrow -\infty$  as  $q \rightarrow 0$ . Hence, the first hybrid mode also extends down to  $\omega=0$ .

c)  $n \geq 2$

In the case of all higher modes, the pertinent approximation is

$$\frac{K_n'(q)}{qK_n(q)} \approx -\frac{1}{q^2} \left[ n + \frac{q^2}{2(n-1)} \right] \quad (n \geq 2),$$

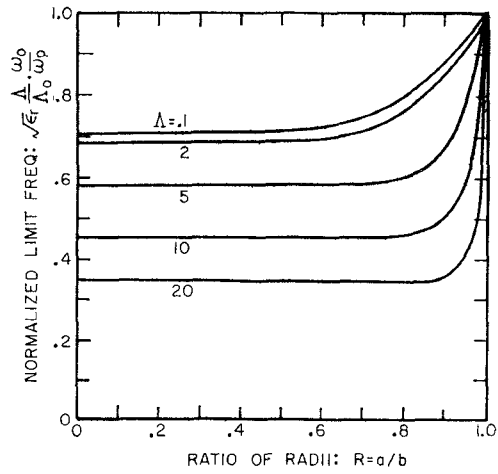


Fig. 7—Plot of the limit frequency  $\omega_0$  for the second hybrid mode ( $n=2$ ) in terms of the plasma guide parameters.

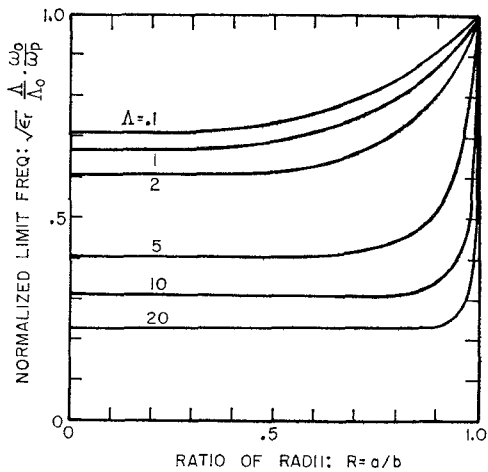


Fig. 8—Plot of the limit frequency  $\omega_0$  for the third hybrid mode ( $n=3$ ) in terms of the plasma guide parameters.

which, when introduced into (10), yields

$$\frac{\epsilon_p}{\epsilon_r} \rightarrow -\frac{\frac{\Lambda}{n-1} + \frac{n}{\Lambda} + \frac{\gamma_4(\Lambda)}{\gamma_2(\Lambda)}}{\frac{n}{\Lambda} + \frac{\gamma_3(\Lambda)}{\gamma_1(\Lambda)}}.$$

Hence, propagation extends down to a *finite* limit frequency, as determined from the last equation. Since the  $\gamma(\Lambda)$  functions vary slowly with  $R$ , except near  $R=1$ , these limit frequencies are very close to those obtained for the plasma column (with no metal rod). This effect is illustrated in Figs. 7 and 8 for  $n=2$  and  $n=3$ , respectively.

These curves also give a measure of the propagation bandwidth obtainable in the higher modes since for  $\Lambda \leq 5$ , this band lies very closely between the values of  $\omega_0$  obtained here and  $\omega_2 = \omega_p(1 + \epsilon_r)^{-1/2}$ .

### ACKNOWLEDGMENT

The authors wish to express their thanks to L. Almeleh for programming and carrying out the numerical work on the IBM-650 computer.